HHS Public Access

Author manuscript

Epilepsia. Author manuscript; available in PMC 2016 November 01.

Published in final edited form as:

Epilepsia. 2015 November ; 56(11): 1819–1827. doi:10.1111/epi.13186.

Segmentation of the Thalamus Based on BOLD Frequencies Affected in Temporal Lobe Epilepsy

Victoria L. Morgan, Ph.D.[1], **Baxter P. Rogers, Ph.D.**[1], and **Bassel Abou-Khalil, M.D.**[2]

[1]Vanderbilt University Institute of Imaging Science, Department of Radiology and Radiological Sciences, Vanderbilt University, Nashville, TN, USA

[2]Department of Neurology, Vanderbilt University, Nashville, TN, USA

Abstract

Objective—Temporal lobe epilepsy is associated with functional changes throughout the brain, particularly including a putative seizure propagation network involving the hippocampus, insula and thalamus. We identified a specified frequency range where functional connectivity in this network was related to duration of disease. Then, to identify specific thalamic nuclei involved in seizure propagation, we determined the subregions of the thalamus that have increased resting functional oscillations in this frequency range.

Methods—Resting-state functional MRI (fMRI) was acquired from twenty unilateral TLE (14 right, 6 left) patients and twenty healthy controls who were each age and gender matched to a specific patient. Wavelet based functional MRI connectivity mapping across the network was computed at each frequency to determine those frequencies where connectivity significantly decreases with duration of disease consistent with impairment due to repeated seizures. The voxel-wise power of the spontaneous blood oxygenation fluctuations of this frequency band was computed in the thalamus of each subject.

Results—Functional connectivity was impaired in the proposed seizure propagation network over a specific range (0.0067–0.013 Hz and 0.024–0.032 Hz) of blood oxygenation oscillations. Increased power in this frequency band (<0.032 Hz) was detected bilaterally in the pulvinar and anterior nucleus of the thalamus of healthy controls, and was increased over the ipsilateral thalamus compared to the contralateral thalamus in TLE.

Significance—This study identified frequencies of impaired connectivity in a TLE seizure propagation network and used them to localize the anterior nucleus and pulvinar of the thalamus as subregions most susceptible to TLE seizures. Further examinations of these frequencies in healthy and TLE subjects may provide unique information relating to the mechanism of seizure propagation and potential treatment using electrical stimulation.

Corresponding Author: Victoria L. Morgan, Ph.D., Vanderbilt University Institute of Imaging Science, 1161 21st Avenue South, AA 1105 MCN, Vanderbilt University, Nashville, TN, USA 37232-2310, Phone: (615)343-5720 Fax: (615)322-0734, victoria.morgan@vanderbilt.edu.

Disclosures

None of the authors has any conflict of interest to disclose. We confirm that we have read the Journal's position on issues involved in ethical publication and affirm that this report is consistent with those guidelines.

Keywords

Functional neuroimaging; fMRI; Temporal lobe epilepsy; Thalamus

Introduction

Identifying and investigating the network of seizure propagation across the brain in focal epilepsy is a difficult but significant challenge. Understanding this network may provide insight into seizure mechanisms in order to understand their behavioral and cognitive effects, and to aid in the development of more specific treatments. In previous work,[1] we have investigated a proposed seizure propagation network including the hippocampus, insula and thalamus ipsilateral to the seizure focus in a population of unilateral temporal lobe epilepsy (TLE) patients using functional MRI (fMRI) resting-state functional connectivity mapping.[2, 3] We found that the difference in functional connectivity across this network between the TLE patient and an age and gender matched healthy control subject changed linearly with duration of disease. Specifically, for durations less than approximately 20 years, the TLE patients had greater functional connectivity within this network than their matched control subject. This difference decreased linearly over time so that those TLE patients with the longest durations of approximately 40 years had a much lower functional connectivity within this network than the matched controls. This relationship supports the idea that the insula [4–8] and thalamus,[9–14] are important nodes in the seizure propagation network in TLE of hippocampal origin.

Functional connectivity mapping measures the synchronicity of low frequency blood oxygenation fluctuations between two fMRI time series in the brain.[2, 3] This measurement is generally confined to and averaged over frequencies less than 0.1 Hz [15] reflecting known periods of spontaneous oscillations in cerebral oxygenation measured with near infrared spectroscopy (NIRS).[16] Wavelet coherence, a method borrowed from oceanography research [17] and recently applied to resting-state functional connectivity mapping,[18] allows interrogation of functional connectivity across the time and frequency domains, where traditional functional connectivity does not. Therefore, we used this method to determine the contribution of specific frequencies of functional connectivity to the correlation between functional connectivity and duration of disease in the ipsilateral hippocampus-insula-thalamus network. We hypothesize that there exists a subset of frequencies within the typical 0.01–0.1Hz range that have an increased contribution over other frequencies, indicating that they are specifically involved in seizure propagation in TLE in this network. Further, we believe that the power of the spontaneous hemodynamic oscillations at these specific frequencies may delineate regions of increased propagation susceptibility within nodes of the network. Therefore, we segmented the thalamus into regions of increased power at these frequencies to identify subregions that are most susceptible to the seizure propagation.

Methods

Subjects

Twenty-two unilateral TLE patients were recruited for this study, with 20 completing the entire imaging procedure (See Table 1). Localization of the epileptogenic zone was based on standard presurgical evaluation, including structural imaging with MRI, ictal and interictal EEG, analysis of seizure semiology, and functional imaging with PET. To create a homogeneous group of mesial TLE subjects, no patients with structural abnormalities other than hippocampal sclerosis were included. Those with bilateral hippocampal sclerosis, but otherwise unilateral findings on presurgical evaluation were included. Note that in patients without hippocampal sclerosis on presurgical MRI, gliosis was identified via resection pathology. In addition, 20 healthy controls with no history of head trauma or neurological or neuropsychological disease were also enrolled. Each individual control subject was age (± 3 years) and gender matched to a TLE patient.

Imaging

Informed consent was obtained prior to scanning each subject per Vanderbilt University Institutional Review Board guidelines. The imaging was performed with a Philips Achieva 3T MRI scanner (Philips Healthcare, Best, Netherlands) using a 32-channel head coil. The acquisition included the following scans: 1) Three-dimensional, T1-weighted whole-brain image series for inter-subject normalization and tissue segmentation (Gradient echo, TR = 9.1 msec, TE = 4.6 ms, 192 shots, flip angle = 8 degrees, matrix = 256x256, 1 x 1 x 1 mm^3), 2) Two-dimensional, T1-weighted axial whole- brain image series in the same slice locations as the fMRI scan for functional to structural data coregistration (1 x 1 x 4 mm^3), and 3) fMRI Blood Oxygenation Level Dependent (BOLD) image series at rest with eyes closed – 80x80, FOV = 240 mm, 30 axial slices, TE = 35 ms, TR = 2 sec, slice thickness = 3.5 mm/0.5 mm gap, 2 x 300 volumes (20 minutes). Physiological monitoring of cardiac and respiratory fluctuations was performed at 500 Hz using the MRI scanner integrated pulse oximeter and the respiratory belt.

Image Preprocessing

Functional MRI images were preprocessed with SPM8 software [http://www.fil.ion.ucl.ac.uk/spm/software/spm8/] and Matlab (The MathWorks, Inc, Natick, MA). All fMRI images were corrected for slice acquisition timing differences and motion artifacts, and the motion time series were saved. The maximum subject translation was compared between groups using a two-sample t-test. Physiological noise correction was then performed using a RETROICOR protocol [19] using the pulse oximeter and respiratory belt time series. The corrected fMRI images were spatially normalized to the Montreal Neurological Institute (MNI) template using the two structural image sets. First, the two-dimensional T1-weighted image was co-registered to the three-dimensional T1-weighted image. Then the three-dimensional T1-weighted image was spatially normalized to the template and the coregistration and normalization parameters were applied to the fMRI images. Next, the fMRI images were spatially smoothed using a 6 x 6 x 6 mm^3 full width, half maximum Gaussian kernel. The normalized fMRI time series were temporally band-pass filtered at 0.0067 Hz to 0.1 Hz[15] for functional connectivity analyses. The temporal

signal to noise ratio (tSNR) of this time series was computed as the mean over time divided by the standard deviation over time. The tSNR of the subjects in the control group were compared to the TLE group using a two-sample t-test. In addition, the spatially normalized three-dimensional, T1-weighted image was segmented into its gray matter, white matter and cerebrospinal fluid components. The average time series over all white matter voxels was computed for use as a confound for the functional connectivity analyses.

Three regions of interest were identified for this study – the hippocampus (HIPI), insula (INSI) and thalamus (THALI) – ipsilateral to the seizure focus in the TLE patients. The ipsilateral side in each control subject was determined as the same as their matched TLE patient. These three regions were identified on the three-dimensional, T1-weighted images using FreeSurfer software.[20, 21] The regions were then transformed to the fMRI images using the transformation matrices determined above. The fMRI time series across all voxels in each of the three regions were averaged for a single time series per region per subject. The average white matter time series and six motion time series for each subject were then regressed from the regional time series. These preprocessed time series for each region in each subject were used in the wavelet coherence analysis of functional connectivity. The FreeSurfer volume of the ipsilateral and contralateral hippocampus was also determined and their ratio was computed for each subject.

Wavelet coherence

In order to examine the frequency dependent functional connectivity, we determined the wavelet coherence of two time series as demonstrated by Chang and Glover[18], utilizing the algorithms developed by Grinstead et al.[17] (available at noc.ac.uk/using-science/crosswavelet-wavelet-coherence) to study geophysical time series. The algorithms are designed to identify regions in time-frequency space with large common power and phase which we attribute to coherence or connectivity between the series. As in [18], we implemented the cross wavelet transform (CWT) to calculate the wavelet coherence between two time series using the default values of the Morlet wavelet with the spacing between discrete octaves set to 0.083 which yielded 81 tested frequencies between 0 and 0.24 Hz. This method repeatedly convolves each time series with scaled and translated wavelet functions to decompose the time series into time-frequency space. The magnitude of the common power or coherence between two time series in this time-frequency space is the cross-wavelet power (R^2), whereas the relative phase between the two is the cross-wavelet phase (θ). Figure 1 shows an example of a CWT plot for the INSI and THALI of a TLE patient using the Morlet wavelet CWT.

In order to translate the CWT information into a measure relatable to traditional functional connectivity (a linear correlation coefficient ranging from 0 to 1 incorporating both magnitude and phase of the relationship), we defined a wavelet functional connectivity (WFC) measure as

$$\mathrm{WFC}(\mathrm{f},\mathrm{t}) = \mathrm{R}^2(\mathrm{f},\mathrm{t}) * \mathrm{real}(\mathrm{e}^{\mathrm{i}\theta(\mathrm{f},\mathrm{t})}) \quad (1)$$

Like a correlation coefficient, this measure has a range between −1 and 1 and incorporates magnitude and phase. We then converted to a Z statistic using the Fisher Z transform. [22] This measure was computed for each pair of regions (HIPI-INSI, HIPI-THALI, INSI-THALI) and averaged to yield a single wavelet functional connectivity time/frequency matrix over the entire defined ipsilateral temporal network (IWFC(f,t)) for each subject.

To verify that this measure corresponds to the traditional functional connectivity, we averaged the IWFC across all frequencies (between 0.0067 and 0.1 Hz) (rows in Figure 1) and time (columns of Figure 1) for each subject. We have previously reported that in a subset of 12 of these subjects, the difference in functional connectivity between each patient and their age and gender matched control (pat-con) linearly correlated with duration of disease ($p=0.03$).[1] The linear correlation between this frequency and time averaged IWFC (pat-con) and duration of disease was computed and compared to the correlation between the traditional functional connectivity (pat-con) and duration of disease across subjects. The traditional functional connectivity was determined by taking the same preprocessed regional time series used in the wavelet coherence analyses and performing a Pearson's linear correlation between the three pairs of regions in each subject, converting to a Z statistic [22] and averaging them. The linear correlation between the time and frequency averaged IWFC and the traditional FC was also determined.

After demonstrating the frequency and time averaged IWFC and its relation to duration of disease, the IWFC(f,t) was averaged across time to compute a series of IWFC(f) for each subject (one number for each frequency or row in Figure 1). The Pearson correlation between IWFC(f) (pat-con) and duration of disease across subjects was computed for each frequency. Frequencies for which the correlation to duration of disease was statistically significant ($p < 0.05$) were determined.

Frequency segmentation

After the determination of the specific frequencies most responsible for the association between functional connectivity and duration of disease, we performed a voxel-wise segmentation of the thalamus based on the power of its resting BOLD oscillations at these frequencies to identify regions that are most susceptible to seizure propagation. The preprocessed fMRI data including slice timing correction, motion correction, physiological noise correction, spatial normalization to the MNI template and spatial smoothing were used. The motion and white matter time series were linearly regressed from the time series and then the Fast Fourier Transform was used to transform the series into the frequency domain. Similar to the amplitude of low frequency fluctuation (ALFF) procedure to determine power in fMRI BOLD oscillations,[23, 24] the square root of the power spectrum was averaged over the frequency of interest (Fi) and over the rest of the frequencies between the 0.0067–0.1 Hz band (Fo). The measure Fi/Fo was used as a marker of the relative power in the frequency of interest. A voxel-wise spatial parametric map of this measure in the thalamus was obtained for each subject. This frequency ratio parametric map was averaged across all subjects in each of the three groups (controls, left TLE, right TLE). Also, to investigate laterality of this frequency ratio, the average of this value across all voxels in the

ipsilateral thalamus was compared to the contralateral thalamus using a paired t-test. This was performed in controls and TLE patients separately.

Results

The maximum motion between the controls and TLE patients were not significantly different as determined by the t-test (controls: 1.08±0.59 mm; TLE: 1.48±0.87 (SD) mm; $p > 0.05$). The tSNR of the fMRI series between the two groups also was not statistically different (controls: 146±23; TLE: 145±32 (SD) mm; $p > 0.05$). The ipsilateral to contralateral hippocampal volume ratio for each subject is included in Table 1. All patients whose ratio is less than two standard deviations from the mean of the 20 controls (mean ± st dev = 1.01 ± 0.04 mm^3) is indicated in BOLD.

The comparison between the frequency and time averaged IWFC and the traditional FC measure is given in Figure 2A. While the traditional values are larger than the IWFC values, the two are significantly correlated ($r = 0.828$, $p < 0.0001$) and the linear relationship to duration of disease remains (Figure 2B, $r = -0.505$, $p = 0.02$). It should be noted that while the network as a whole demonstrates this linear relationship with duration of disease, the individual paths of the network do not (HIPI-THALI $r = -0.36$, p = 0.10; HIPI-INSI $r = -0.24$, $p = 0.30$; THALI-INSI $r = -0.47$, $p = 0.03$).

The IWFC(f) analysis showed that at frequencies of 0.0067–0.013 Hz and 0.024–0.032 Hz the IWFC (pat-con) was significantly correlated with duration of disease (Figure 3A). When only these frequencies are used to compute the IWFC, the correlation with duration of disease is highly significant ($r = -0.683$, $p < 0.001$), as expected (Figure 3B).

For the frequency segmentation, the frequency band of interest (Fi) was chosen as 0.0067 to 0.032 Hz to be a continuous band including all frequencies that showed a significant correlation between IWFC(f) and duration of disease (blue line Figure 3A). The other frequencies (Fo, red line Figure 3A) were then 0.032 to 0.1 Hz. The ratio of the power of the resting fMRI BOLD oscillations for each voxel in the thalamus for these two frequency bands was generally between 1.2 and 1.8. Figure 4 shows the spatial distribution of the average of this ratio across the control group with increases in the pulvinar and anterior nucleus regions bilaterally.

Figure 5 shows that the average of this ratio across the left TLE and right TLE patients is increased ipsilateral to the seizures, but with a less focal distribution pattern. When averaged across the thalamus in each subject, the average frequency ratio across the ipsilateral thalamus was increased over the contralateral thalamus in the TLE subjects ($p = 0.02$), but not controls.

Discussion

In this work we investigated the frequency characteristics of the functional connectivity of the proposed seizure propagation network in TLE. First, we demonstrated that the functional connectivity within this network is impaired as compared with healthy controls and decreases with increased duration of disease. This is supported in part by Bettus et al. [25] who

found decreased ipsilateral connectivity and increased contralateral connectivity in TLE, although they investigated regions more proximal to the hippocampus. We then identified that frequencies of 0.0067–0.013 Hz and 0.024–0.032 Hz are most responsible for this functional connectivity impairment over time. Second, we determined that in the thalamus of healthy controls, spontaneous resting blood oxygenation fluctuations within the 0.0067–0.032 Hz range have increased power compared to the 0.032–0.1 Hz range in the pulvinar and anterior nucleus regions bilaterally. Across the TLE patients, this increase was less focal but greater in the ipsilateral hemisphere. These findings suggest these regions are most susceptible to functional connectivity impairment from TLE seizures.

The pulvinar of the thalamus is known to be involved in TLE seizures. Electrographically, Rosenberg et al.[26] showed that the pulvinar was involved with 79.7% of 74 unifocal seizures recorded in 14 patients with refractory TLE who had intracerebral electrodes placed in the medial pulvinar in the thalamus. In these data the medial pulvinar was more frequently involved in the ictal process when the seizures originated in the mesial temporal structures, as suspected in our cohort, rather than lateral neocortex; and was always involved when propagation between mesial and lateral structures occurred. In another EEG study of 13 TLE patients, thalamic involvement occurred in all seizures originating from the mesial temporal structures.[27] The placement of the thalamic electrode was variable across subjects in this cohort, but was located in the pulvinar in 8 of the 13 patients. No comparison was made between results yielded from different electrode placement.

The anterior nucleus of the thalamus has been the site of several investigations of electrical stimulation for the treatment of intractable focal epilepsy.[28, 29] The largest of these is the controlled clinical trial of stimulation of the anterior nuclei of the thalamus for epilepsy (SANTE).[30] This study included 110 patients undergoing bilateral implantation of electrodes in the anterior nucleus of the thalamus. In the subset of TLE subjects (60% of the group), there was a 44.2% median seizure reduction with stimulation compared to 21.8% in the control group (p= 0.025). Interestingly, those with frontal, parietal or occipital seizures had no significant changes in seizures with stimulation.

The thalamic frequency map is also comparable to profiles of thalamic structural atrophy in TLE. In a study of shape characteristics using a point-wise analysis of T1-weighted MRI in TLE patients with hippocampal sclerosis, Bernhardt et al.[12] showed a pattern of ipsilateral mesial thalamic thinning in TLE compared to controls. The thinning was predominant in the posterior and anterior mesial regions and was linearly related to duration of disease, but not age. A similar pattern of exclusively posterior thalamic atrophy was also reported by Keller et al. [31] in TLE.

Using diffusion sensitive MRI and tractography processing methods it is possible to parcellate the thalamus by the cortical regions in which the white matter tracts of a given voxel terminate. Using this structural connectivity in healthy controls the pulvinar region connections have been mapped to the temporal and parietal lobe cortex.[32, 33] The structural connectivity (number of streamlines) between this region of the ipsilateral thalamus and temporal lobe is reduced [31] in both left and right TLE. When the thalamus is parcellated by structural connectivity to the amygdala, entorhinal cortex, hippocampus, and

parahippocampus, the pulvinar showed the highest density of connections to the hippocampus in controls and TLE.[13]

Taken together, this evidence supports our results that the pulvinar and anterior nucleus of the thalamus are part of a functional network including the ipsilateral insula and hippocampus and are affected by temporal lobe epilepsy. However, the role of the specific frequency range 0.0067–0.032 Hz remains unclear. Infra-slow (<0.1 Hz) neuronal oscillations in the brain are believed to be created by long-lasting rhythmic hyperpolarizing potentials [34] relevant to communication across functional networks in healthy subjects [35, 36] and in epilepsy.[37, 38] Oscillations in fMRI BOLD signal, like those measured in functional connectivity, are believed to stem from the same underlying physiological neuronal phenomena as these EEG signals.[39] Infra-slow EEG oscillations have been found to correlate with fMRI BOLD signals in known resting state networks,[40–42] but no specific evidence supporting the frequencies <0.032 Hz detected in our study was found. However, the increased power of spontaneous BOLD oscillations in the 0.0067–0.032 Hz range in the ipsilateral compared to the contralateral thalamus in the TLE subjects (Figure 5) further supports the increased relative contribution of these frequencies in TLE seizures. The less focal distribution of these oscillations in the ipsilateral thalamus when averaged across the population of TLE patients suggests variability across patients which may partially reflect an evolution over years of disease duration.

While we used the frequencies determined from the network analysis to segment only one node in this work, it may be possible to use a similar approach to investigate the spatial patterns of the hippocampus and insula as well. However, the spatial resolution of our fMRI images did not provide identifiable or distinct spatial patterns in these smaller, thinner regions. This issue is confounded in the hippocampus by the more severe structural changes in this region in these patients.

One limitation of this study is the inclusion of TLE patients with and without hippocampal sclerosis. By qualitative clinical assessment of the clinical MRI, four patients did not have hippocampal sclerosis (#6, 7, 11, 22). By volumetric analysis of the research 3D T1-weighted MRI, five patients did not have hippocampal sclerosis (#2, 11, 16, 17, 22). In the literature, there is evidence of unique patterns of functional epileptogenic networks between TLE patients with and without hippocampal sclerosis, [43] in addition to white matter differences between the groups. [44] Postmortem pathology revealed changes in the thalamus of TLE patients that differed between those with and without hippocampal sclerosis. [45] These differences would increase variability in the presented work. However, fMRI activation resulting from interictal spikes have been detected in the ipsilateral anterior temporal lobe and insula in both patients with and without hippocampal sclerosis [46]. And, thalamic volume loss was also measured in both types of patients. [47] This suggests that our choice of an ipsilateral epileptogenic network including the hippocampus, insula and thalamus is appropriate for all patients in this study.

In conclusion, fMRI was used to identify functional connectivity over a specific range (0.0067–0.032 Hz) of BOLD oscillations that is impaired over time in a proposed seizure propagation network in TLE. Increased power in this frequency band was used to identify

the pulvinar and anterior nucleus of the thalamus of healthy controls as those subregions most susceptible to epileptic seizures and related functional connectivity impairment. While there is considerable support for the validity of the role of these thalamic regions in TLE and their healthy connections to the temporal lobe, frequency dependent segmentation of this structure is novel. Further examinations of these frequencies in healthy and TLE subjects may provide unique information relating to the mechanism of seizure propagation and potential treatment using electrical stimulation.

Acknowledgments

The authors thank Benjamin Conrad for his contribution in coordinating the data acquisition for this study. The authors also thank Robert Barry, Ph.D. for providing the algorithm for the RETROICOR physiological noise correction of the fMRI images. This study was supported by NIH R01 NS075270 (VLM).

References

1. Morgan VL, Abou-Khalil B, Rogers BP. Evolution of Functional Connectivity of Brain Networks and Their Dynamic Interaction in Temporal Lobe Epilepsy. Brain Connect. 2014
2. Rogers BP, Morgan VL, Newton AT, et al. Assessing functional connectivity in the human brain by fMRI. Magn Reson Imaging. 2007; 25:1347–57. [PubMed: 17499467]
3. Biswal B, Yetkin FZ, Haughton VM, et al. Functional connectivity in the motor cortex of resting human brain using echo-planar MRI. Magn Reson Med. 1995; 34:537–41. [PubMed: 8524021]
4. Blauwblomme T, David O, Minotti L, et al. Prognostic value of insular lobe involvement in temporal lobe epilepsy: A stereoelectroencephalographic study. Epilepsia. 2013; 54:1658–1667. [PubMed: 23848549]
5. Isnard J, Guenot M, Ostrowsky K, et al. The role of the insular cortex in temporal lobe epilepsy. Ann Neurol. 2000; 48:614–23. [PubMed: 11026445]
6. Chassoux F, Semah F, Bouilleret V, et al. Metabolic changes and electro-clinical patterns in mesio-temporal lobe epilepsy: a correlative study. Brain. 2004; 127:164–74. [PubMed: 14534161]
7. Kim BJ, Hong SB, Seo DW. Differences in ictal hyperperfusion of limbic-related structures between mesial temporal and neocortical epilepsy. Epilepsy Res. 2008; 81:167–75. [PubMed: 18639441]
8. Maccotta L, He BJ, Snyder AZ, et al. Impaired and facilitated functional networks in temporal lobe epilepsy. Neuroimage Clin. 2013; 2:862–72. [PubMed: 24073391]
9. Yu L, Blumenfeld H. Theories of impaired consciousness in epilepsy. Disorders of Consciousness. 2009; 1157:48–60.
10. Blumenfeld H, Varghese GI, Purcaro MJ, et al. Cortical and subcortical networks in human secondarily generalized tonic-clonic seizures. Brain. 2009; 132:999–1012. [PubMed: 19339252]
11. Englot DJ, Mishra AM, Mansuripur PK, et al. Remote effects of focal hippocampal seizures on the rat neocortex. J Neurosci. 2008; 28:9066–81. [PubMed: 18768701]
12. Bernhardt BC, Bernasconi N, Kim H, et al. Mapping thalamocortical network pathology in temporal lobe epilepsy. Neurology. 2012; 78:129–36. [PubMed: 22205759]
13. Barron DS, Tandon N, Lancaster JL, et al. Thalamic structural connectivity in medial temporal lobe epilepsy. Epilepsia. 2014; 55:e50–e55. [PubMed: 24802969]
14. Barron DS, Fox PT, Pardoe H, et al. Thalamic functional connectivity predicts seizure laterality in individual TLE patients: Application of a biomarker development strategy. NeuroImage: Clinical. 2015; 7:273–280. [PubMed: 25610790]
15. Cordes D, Haughton VM, Arfanakis K, et al. Frequencies contributing to functional connectivity in the cerebral cortex in “resting-state” data. AJNR Am J Neuroradiol. 2001; 22:1326–33. [PubMed: 11498421]
16. Obrig H, Neufang M, Wenzel R, et al. Spontaneous low frequency oscillations of cerebral hemodynamics and metabolism in human adults. Neuroimage. 2000; 12:623–39. [PubMed: 11112395]

17. Grinsted A, Moore JC, Jevrejeva S. Application of the cross wavelet transform and wavelet coherence to geophysical time series. Nonlin Processes Geophys. 2004; 11:561–566.
18. Chang C, Glover GH. Time-frequency dynamics of resting-state brain connectivity measured with fMRI. Neuroimage. 2010; 50:81–98. [PubMed: 20006716]
19. Glover GH, Li TQ, Ress D. Image-based method for retrospective correction of physiological motion effects in fMRI: RETROICOR. Magn Reson Med. 2000; 44:162–7. [PubMed: 10893535]
20. Dale AM, Fischl B, Sereno MI. Cortical surface-based analysis - I. Segmentation and surface reconstruction. Neuroimage. 1999; 9:179–194. [PubMed: 9931268]
21. Fischl B, van der Kouwe A, Destrieux C, et al. Automatically parcellating the human cerebral cortex. Cerebral Cortex. 2004; 14:11–22. [PubMed: 14654453]
22. Fisher RA. Frequency Distribution of the Values of the Correlation Coefficient in Samples from an Indefinitely Large Population. Biometrika. 1915; 10:507–521.
23. Zhang J, Wei L, Hu X, et al. Specific frequency band of amplitude low-frequency fluctuation predicts Parkinson's disease. Behavioural Brain Research. 2013; 252:18–23. [PubMed: 23727173]
24. Yang H, Long XY, Yang YH, et al. Amplitude of low frequency fluctuation within visual areas revealed by resting-state functional MRI. Neuroimage. 2007; 36:144–152. [PubMed: 17434757]
25. Bettus G, Bartolomei F, Confort-Gouny S, et al. Role of resting state functional connectivity MRI in presurgical investigation of mesial temporal lobe epilepsy. Journal of Neurology Neurosurgery and Psychiatry. 2010; 81:1147–1154.
26. Rosenberg DS, Mauguiere F, Demarquay G, et al. Involvement of medial pulvinar thalamic nucleus in human temporal lobe seizures. Epilepsia. 2006; 47:98–107. [PubMed: 16417537]
27. Guye M, Regis J, Tamura M, et al. The role of corticothalamic coupling in human temporal lobe epilepsy. Brain. 2006; 129:1917–28. [PubMed: 16760199]
28. Kerrigan JF, Litt B, Fisher RS, et al. Electrical stimulation of the anterior nucleus of the thalamus for the treatment of intractable epilepsy. Epilepsia. 2004; 45:346–354. [PubMed: 15030497]
29. Lim SN, Lee ST, Tsai YT, et al. Electrical stimulation of the anterior nucleus of the thalamus for intractable epilepsy: A long-term follow-up study. Epilepsia. 2007; 48:342–347. [PubMed: 17295629]
30. Fisher R, Salanova V, Witt T, et al. Electrical stimulation of the anterior nucleus of thalamus for treatment of refractory epilepsy. Epilepsia. 2010; 51:899–908. [PubMed: 20331461]
31. Keller SS, O'Muircheartaigh J, Traynor C, et al. Thalamotemporal impairment in temporal lobe epilepsy: a combined MRI analysis of structure, integrity, and connectivity. Epilepsia. 2014; 55:306–15. [PubMed: 24447099]
32. Johansen-Berg H, Behrens TEJ, Sillery E, et al. Functional-anatomical validation and individual variation of diffusion tractography-based segmentation of the human thalamus. Cerebral Cortex. 2005; 15:31–39. [PubMed: 15238447]
33. Traynor C, Heckemann RA, Hammers A, et al. Reproducibility of thalamic segmentation based on probabilistic tractography. Neuroimage. 2010; 52:69–85. [PubMed: 20398772]
34. Lorincz ML, Geall F, Bao Y, et al. ATP-Dependent Infra-Slow (< 0. 1 Hz) Oscillations in Thalamic Networks. Plos One. 2009; 4:e4447. [PubMed: 19212445]
35. Buzsáki G, Draguhn A. Neuronal Oscillations in Cortical Networks. Science. 2004; 304:1926–1929. [PubMed: 15218136]
36. Monto S, Palva S, Voipio J, et al. Very slow EEG fluctuations predict the dynamics of stimulus detection and oscillation amplitudes in humans. Journal of Neuroscience. 2008; 28:8268–8272. [PubMed: 18701689]
37. Rodin E, Constantino T, Bigelow J. Interictal infraslow activity in patients with epilepsy. Clinical Neurophysiology. 2014; 125:919–929. [PubMed: 24239456]
38. Vanhatalo S, Palva JM, Holmes MD, et al. Infraslow oscillations modulate excitability and interictal epileptic activity in the human cortex during sleep. Proceedings of the National Academy of Sciences of the United States of America. 2004; 101:5053–5057. [PubMed: 15044698]
39. Palva JM, Palva S. Infra-slow fluctuations in electrophysiological recordings, blood-oxygenation-level-dependent signals, and psychophysical time series. Neuroimage. 2012; 62:2201–2211. [PubMed: 22401756]

40. Hiltunen T, Kantola J, Abou Elseoud A, et al. Infra-Slow EEG Fluctuations Are Correlated with Resting-State Network Dynamics in fMRI. Journal of Neuroscience. 2014; 34:356–362. [PubMed: 24403137]

41. Gohel SR, Biswal BB. Functional integration between brain regions at 'rest' occurs in multiple-frequency bands. Brain Connect. 2014

42. Wu CW, Gu H, Lu H, et al. Frequency specificity of functional connectivity in brain networks. Neuroimage. 2008; 42:1047–55. [PubMed: 18632288]

43. Bernhardt BC, Bernasconi N, Concha L, et al. Cortical thickness analysis in temporal lobe epilepsy Reproducibility and relation to outcome. Neurology. 2010; 74:1776–1784. [PubMed: 20513813]

44. Scanlon C, Mueller SG, Cheong I, et al. Grey and white matter abnormalities in temporal lobe epilepsy with and without mesial temporal sclerosis. Journal of Neurology. 2013; 260:2320–2329. [PubMed: 23754695]

45. Sinjab B, Martinian L, Sisodiya SM, et al. Regional thalamic neuropathology in patients with hippocampal sclerosis and epilepsy: A postmortem study. Epilepsia. 2013; 54:2125–2133. [PubMed: 24138281]

46. Coan AC, Campos BM, Beltramini GC, et al. Distinct functional and structural MRI abnormalities in mesial temporal lobe epilepsy with and without hippocampal sclerosis. Epilepsia. 2014; 55:1187–1196. [PubMed: 24903633]

47. Mueller SG, Laxer KD, Barakos J, et al. Involvement of the thalamocortical network in TLE with and without mesiotemporal sclerosis. Epilepsia. 2010; 51:1436–1445. [PubMed: 20002143]

Key Point Box

- The functional connectivity of the ipsilateral hippocampus, insula and thalamus network changes linearly with duration of TLE.
- The spontaneous blood oxygenation fluctuations at frequencies less than 0.032 Hz are most responsible for this association in that network.
- The power of these fluctuations less than 0.032 Hz is increased bilaterally in the pulvinar and anterior nucleus regions in controls.
- Blood oxygenation oscillations less than 0.032 Hz may be an indicator of seizure susceptibility in TLE.

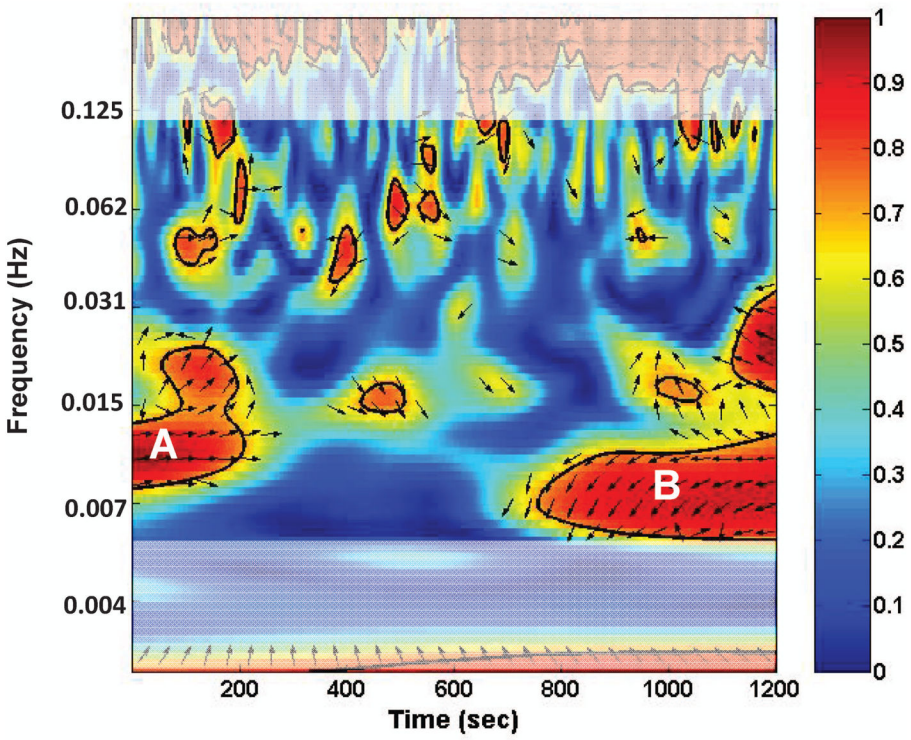

Figure 1.

Example of a cross wavelet transform (CWT) plot for INSI and THALI of a TLE patient using the Morlet wavelet. The R^2 is denoted by color (0–1) and the θ is indicated by the direction of the arrow. The white shading represents frequencies temporally filtered in the preprocessing for functional connectivity. The horizontal axis is the time during the scan. The vertical axis represents frequency of BOLD oscillations. This example shows that in the first 200 seconds of the scan, the highest connectivity between the two regions occurs at a frequency of approximately 0.01 Hz (A); while later in the last 400 seconds of the scan, the highest correlation occurs at a frequency of about 0.007 Hz (B).

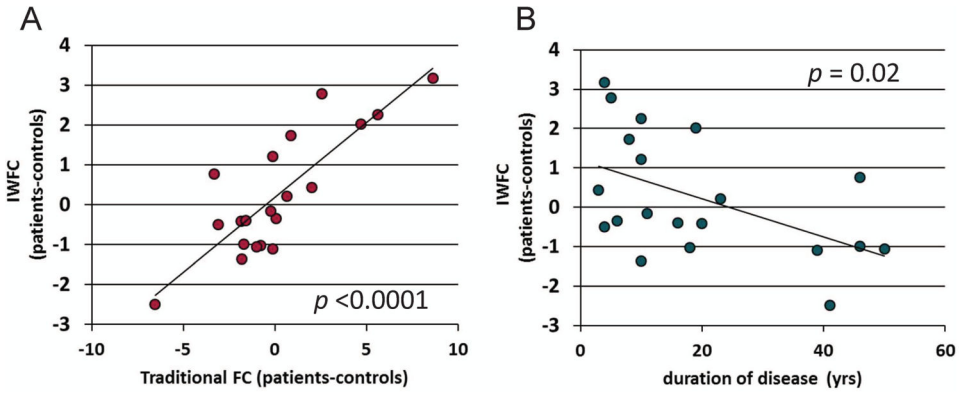

Figure 2.

Validation of IWFC(f,t) measure. (A) Frequency and time averaged IWFC vs. traditional FC. (B) Frequency and time averaged IWFC vs. duration of disease. Solid line represents linear trendline. Each point in (B) represents the IWFC of each patient minus the age and gender matched healthy control (pat-con).

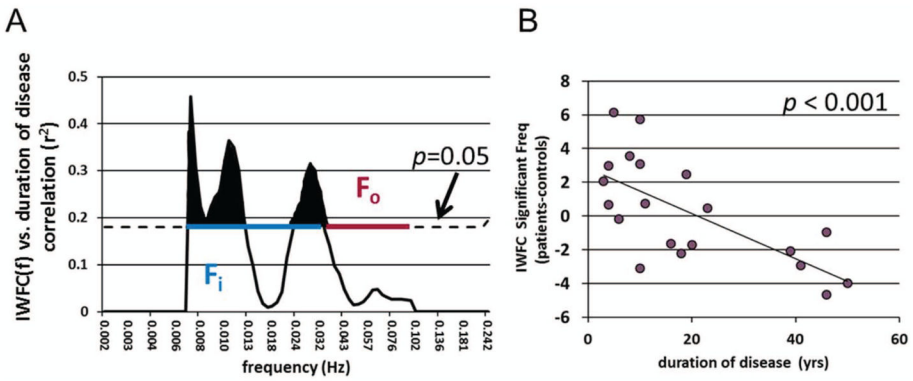

Figure 3.

IWFC(f) frequency analysis. (A) Correlation between IWFC(f) (pat-con) vs. duration of disease at each frequency. Dotted black line indicates r^2 value over which $p < 0.05$. Shaded black areas show frequencies for which this correlation is statistically significant. The blue line represents the frequency band of interest (F_i), while the red line denotes the other frequencies (F_o) used for thalamus segmentation. (B) IWFC averaged only for significant frequencies shown in A (0.0067–0.013 Hz and 0.024–0.032 Hz). Correlation to duration of disease is higher than that of all frequencies shown in Figure 2B ($r = -0.505$ for all frequencies vs. $r = -0.683$ for significant frequencies only). Solid line represents linear trendline. Each point in (B) represents the IWFC of each patient minus the age and gender matched healthy control (pat-con).

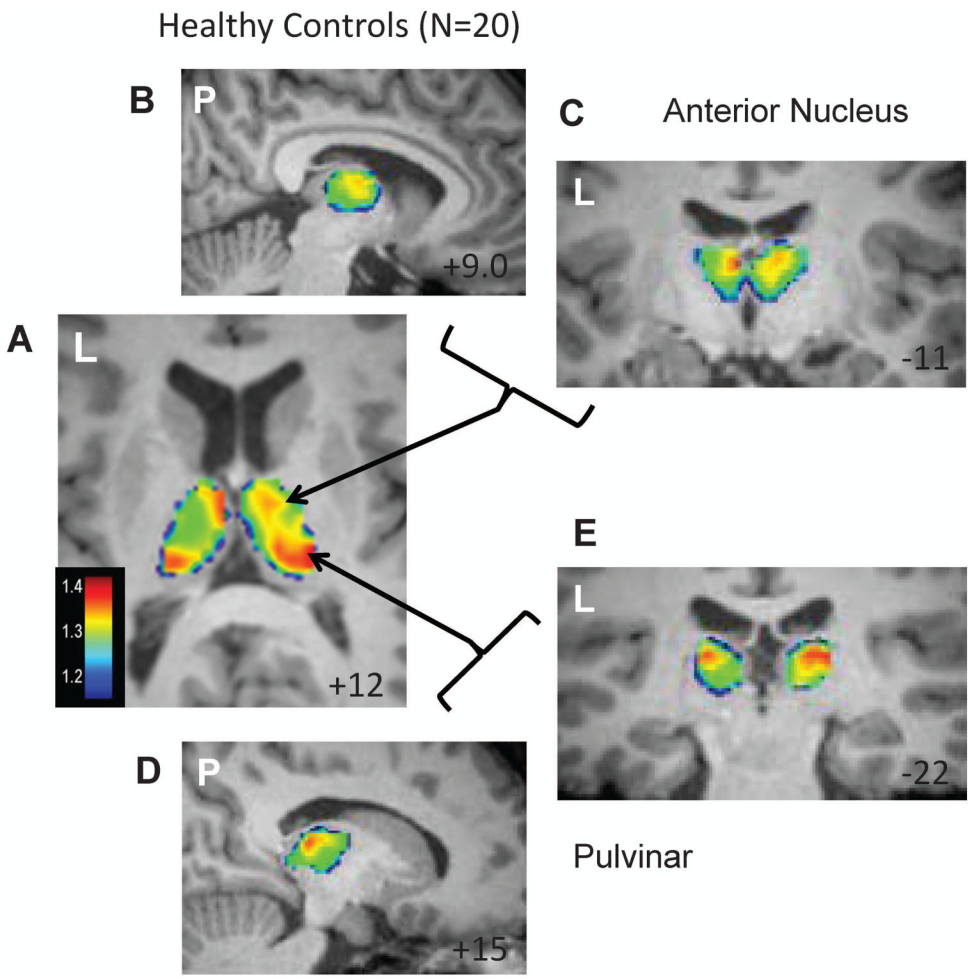

Figure 4.

Frequency segmentation of the thalamus in healthy controls. Average of Fi/Fo power across 20 healthy control subjects. (A) Axial slice showing increased power in bilateral anterior nucleus and pulvinar regions. Increased power in the anterior nucleus region is shown in a sagittal (B) and coronal (C) section. Increased power in the pulvinar region is shown in a sagittal (D) and coronal (E) section. Left (L) or posterior (P) side of the image is indicated in each. MNI template slice location is given in the bottom right corner in mm.

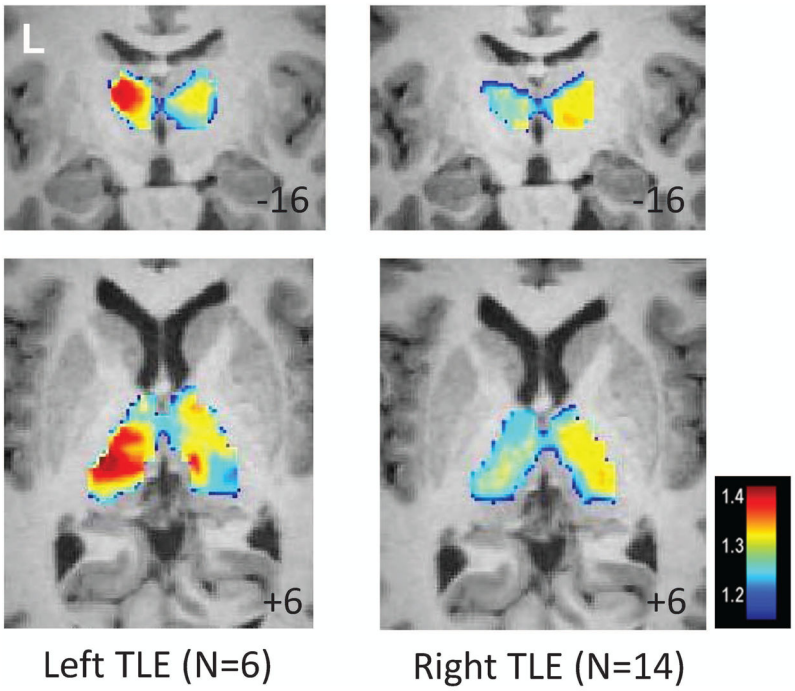

Figure 5.

Frequency segmentation of the thalamus in TLE. Average of Fi/Fo power across 6 left TLE patients (left) and 14 right TLE patients (right). MNI template slice location is given in the bottom right corner in mm.

Table 1

Subject characteristics of patients and matched controls.

Subject ID	Age: patient/control	Gender	Hand: patient/control	Age of Onset (yrs)	Side of TLE	HS	duration (yrs)	HIP volume ratio (I/C) patient/control
2	49/50	F	R/R	30	R	L>R	19	0.97/1.08
3	51/54	F	R/R	10	R	R	41	**0.71**/1.01
4	18/18	F	R/R	1	L	L	17	**0.82**/1.01
5	39/38	F	R/R	0	R	R	39	**0.82**/1.02
6	28/27	M	R/R	24	L	no*	4	**0.93**/0.93
7	54/56	F	R/R	35	R	no*	19	**0.72**/1.09
8	18/18	M	R/R	12	L	L	6	**0.76**/0.97
9	43/41	M	R/R	33	R	R	10	**0.88**/0.97
10	24/23	M	R/R	1	R	L>R	23	**0.59**/1.00
11	23/23	M	L/R	19	R	no*	4	0.95/1.05
12	41/42	F	R/R	23	R	R	18	**0.48**/1.00
13	38/38	F	R/R	33	R	R	5	**0.78**/0.99
14	37/37	F	R/R	34	R	R	3	**0.74**/0.99
15	68/71	M	R/R	18	L	L	50	**0.88**/1.00
16	21/20	M	R/L	13	L	L	8	1.18/0.93
17	38/39	F	R/L	27	R	R	11	1.21/0.95
18	38/37	M	R/R	28	R	R	10	**0.78**/1.06
19	46/45	F	L/R	0	L	L	46	**0.80**/1.05
21	46/46	M	L/R	0	R	R	46	**0.80**/1.05
22	42/42	F	R/L	32	R	no*	10	1.07/0.99

Patients #1 and # 20 did not complete the imaging procedure and are not included in the analyses. HS = side of hippocampal sclerosis interpreted from clinical MRI; no = no sclerosis;

*gliosis determined from surgical pathology; L>R = more sclerosis on left; M = male; F = female; patient and control pairs were same gender. HIP volume = hippocampal volume from FreeSurfer (ratio Ipsi/Contra).

Numbers in BOLD represent those where patient's ratio is less than 2 standard deviations from mean of the 20 control subjects, indicating significant unilateral hippocampal volume decrease ipsilateral to focus. Matched control was ± 3 years from age of patient. Side of TLE is based on standard clinical evaluation.